ELSEVIER

Journal of Non-Crystalline Solids 297 (2002) 96–101

JOURNAL OF
NON-CRYSTALLINE SOLIDS

www.elsevier.com/locate/jnoncrysol

Short-range order in non-stoichiometric amorphous silicon oxynitride and silicon-rich nitride

V.A. Gritsenko [a,*], R.W.M. Kwok [b], Hei Wong [c], J.B. Xu [d]

[a] Institute of Semiconductor Physics, Siberian Branch of Russian Academy of Science, Lavrentiev Ave-13, 630090 Novosibirsk, Russia
[b] Department of Chemistry, The Chinese University of Hong Kong, Shatin, Hong Kong
[c] Department of Electronic Engineering, City U, 83 Tat Chee Avenue, Hong Kong
[d] Department of Electronic Engineering, The Chinese University of Hong Kong, Shatin, Hong Kong

Received 9 March 2001; received in revised form 16 April 2001

Abstract

By de-convoluting the Si 2p X-ray photoelectronic spectra, it was found that the short-range order in amorphous silicon oxynitride (SiO_xN_y) films with different compositions can be quantitatively described by the random bonding model. In this model the SiO_xN_y consists of five types of randomly distributed tetrahedra and it indicates that metal–oxide–semiconductor transistor with this gate dielectric will not result in any gigantic potential fluctuation in the conduction channel. On the contrary, the structure of silicon-rich silicon nitride SiN_x can only be described by the random mixture model where the local composition fluctuations in this film will result in gigantic potential contravariant fluctuation. © 2002 Elsevier Science B.V. All rights reserved.

PACS: 82.80Pv; 73.40.Qv; 73.60.Hy

1. Introduction

In future nanoscale silicon metal–oxide–semiconductor (MOS) devices, the gate dielectric thickness will be further scaled down to less than 4 nm and many dielectric-induced instabilities will result. To meet this challenge, it is proposed that the amorphous thermal gate silicon dioxide (SiO_2) should be replaced by amorphous silicon oxynitride (SiO_xN_y) [1–3] or stacked SiO_2/Si_3N_4 dielectric [4]. Particularly, the oxynitride dielectric, combining the advantages of SiO_2 and amorphous silicon nitride (Si_3N_4) [1], has been investigated extensively and silicon-rich silicon nitride (SiN_x) has been used as in triple $SiO_2/SiN_x/SiO_2$ structures for memory devices [5]. The bonding structure in oxynitride and nitride are quite clear now. The bonding in stoichiometric SiO_xN_y is governed by the Mott rule [6–8]. According to this rule, each Si atom is co-ordinated by four O and/or N atoms, each O atom (as in SiO_2) is co-ordinated by two Si atoms, and each N atom is co-ordinated by three Si or O atoms. These bonds should also form the basic network elements of non-stoichiometric amorphous oxynitride films. However, the composition of the bonds and network structure

* Corresponding author.
E-mail address: grits@isp.nsc.ru (V.A. Gritsenko).

0022-3093/02/$ - see front matter © 2002 Elsevier Science B.V. All rights reserved.
PII: S0022-3093(01)00910-3

for the non-stoichiometric dielectric films are still unclear.

There are two extreme models for modeling the structure of tetrahedral amorphous non-stoichiometric alloys: the random mixture model (RMM) and the random bonding model (RBM). These models have been widely used to describe the structure of tetrahedral SiO_xN_y, non-stoichiometric amorphous silicon oxide (SiO_x) and non-stoichiometric amorphous silicon nitride (SiN_x) [9–19]. According to RMM, the SiO_xN_y film consists of separated SiO_2 and Si_3N_4 phases and the SiN_x film consists of separated Si_3N_4 and Si phases, whereas, in the random bonding model, it is assumed that the SiO_xN_y and SiN_x film consist of a network of five tetrahedra of SiO_vN_{4-v} and SiN_vSi_{4-v} (where $v = 0$, 1, 2, 3 and 4), respectively.

The dielectric constants of SiO_2 and Si_3N_4 are 3.9 and 6.5, respectively. If RMM is the real structure for oxynitride film, the gate oxynitride should be composed of a mixture of SiO_2 and Si_3N_4 nanoclusters; then the gigantic surface potential fluctuations ($q\delta$) will be probably generated by the gate voltage in the vicinity of the channel of MOS devices for very thin gate dielectric film (1–4 nm). The surface potential fluctuation may significantly large than the thermal voltage (kT) and causes several undesirable effects such as carrier mobility degradation. Hence it is essential to understand the short-range order in SiO_xN_y to have a good gate oxynitride for MOS devices. As only qualitative description of the RBM was reported, this work aims to quantitatively validate the applicability of the RBM or RMM to a ternary alloy SiO_xN_y and to compare with the short-range order properties in SiN_x.

2. Theory

The distribution function of the SiO_vN_{4-v} tetrahedron in SiO_xN_y with composition x and y in RBM is given by [13,14]

$$W(v,x,y) = \left(\frac{2x}{2x+3y}\right)^{v}\left(\frac{3y}{2x+3y}\right)^{4-v} \times \frac{4!}{v!(4-v)!}. \quad (1)$$

Eq. (1) can be used to describe quantitatively the relative probability of the five sorts of SiO_vN_{4-v} tetrahedra in SiO_xN_y. To determine the chemical shift of Si 2p peaks for tetrahedra SiO_4, SiO_3N, SiO_2N_2, $SiON_3$, and SiN_4 in SiO_xN_y, we extended the Hasegawa RBM for binary alloys (SiO_x or SiN_x) [10] to ternary alloy. For a tetrahedron of SiO_vN_{4-v} with bonding unit $Si_kO_mN_n$, the partial charge $P_j(v)$ of atom j can be determined by

$$P_j(v) = (S_{SiON} - S_j)/(2.08 S_j^{1/2}), \quad (2)$$

where $j =$ Si, O or N, and $S_{SiON} = (S_{Si}^k S_O^m S_N^n)^{1/(k+m+n)}$ is the Sanderson electronegativity in the bonding unit of $Si_kO_mN_n$ and the Sanderson electronegativities for Si, O, and N atoms are $S_{Si} = 2.84$, $S_O = 5.21$, and $S_N = 4.49$, respectively [20].

Considering a SiO_xN_y film with composition x and y, the average partial charge at Si, O and N can be calculated as

$$P_{Si}(x,y) = \sum_{v=0}^{4}[P_{Si}(v)W(v,x,y)] \Big/ \sum_{v=0}^{4}[W(v,x,y)], \quad (3)$$

$$P_O(x,y) = \sum_{v=0}^{4} v[P_O(v)W(v,x,y)] \Big/ \sum_{v=0}^{4} v[W(v,x,y)], \quad (4)$$

$$P_N(x,y) = \sum_{v=0}^{4}(4-v)[P_N(v)W(v,x,y)] \Big/ \sum_{v=0}^{4}(4-v)[W(v,x,y)]. \quad (5)$$

Since the chemical shift of Si 2p level for each of the five tetrahedra is proportional to the partial charge on the Si atom, we can use the Si $2p_{3/2}$ position in SiO_2 and Si_3N_4 to determine the Si $2p_{3/2}$ positions of $SiON_3$, SiO_2N_2 and SiO_3N tetrahedra.

3. Results and discussion

The amorphous SiO_xN_y films of different compositions were prepared on silicon $\langle 100 \rangle$ sub-

strates by low-pressure chemical vapour deposition (LPCVD) from SiH_4, NH_3 and O_2 source at 875 °C. The chemical compositions were determined by X-ray photoelectron spectroscopy (XPS). Angle-resolved XPS measurements were used. With this approach, when the detector is normal to the sample surface, the XPS signals are considered as the bulk signals of the dielectric films. Further details of SiO_xN_y film preparation and XPS measurements were reported previously [6]. The SiN_x samples with thickness about 200 Å were produced by LPCVD from a mixture of SiH_2Cl_2 and NH_3 with different ratios at 760 °C on silicon ⟨1 0 0⟩ wafers.

Random bonding simulations of the Si 2p peaks with spin doublet splitting energy of 0.61 eV were conducted for comparison. For all the six measured SiO_xN_y samples, the same values of chemical shifts and full-width half-maximum (FWHM) for the five tetrahedra were used and the calculated binding energies were used as the peak positions. The same approach was also used for the SiN_x spectra simulations.

Fig. 1 shows the Si 2p core level XPS of SiO_xN_y films with different compositions. Experimental spectra are shown in dots and the simulated spectra from RMM (second spectrum) and RBM (except second spectrum) are depicted in solid lines. For SiO_xN_y simulation the chemical shift of SiO_4, SiO_3N, SiO_2N_2, $SiON_3$, and SiN_4 tetrahedra was calculated using Eq. (3), and the assumption that the chemical shift is proportional to charge on the central silicon atom. The experimental FWHM values for Si_3N_4 and SiO_2 are 1.87 and 1.66 eV, respectively (see Fig. 1). FWHM values for SiO_3N, SiO_2N_2, and $SiON_3$ tetrahedra were estimated based on linear interpolation using the number of oxygen atoms as a parameter. Regardless of the different compositions of x and y, only one peak is observed in experimental spectra. These results do not agree with the RMM. According to the RMM, the Si 2p XPS spectrum should have two peaks, corresponding to the SiO_2 and Si_3N_4 phases, respectively (see the second spectrum in Fig. 1). Instead, the RBM can fit the XPS results for all the samples very well. Curves (except the second trace) below the experimental spectra are the components of different tetrahedra (SiO_vN_{4-v}) that make up the solid lines to approximate the experimental spectra. However, the RBM is not applicable to all kinds of dielectric films.

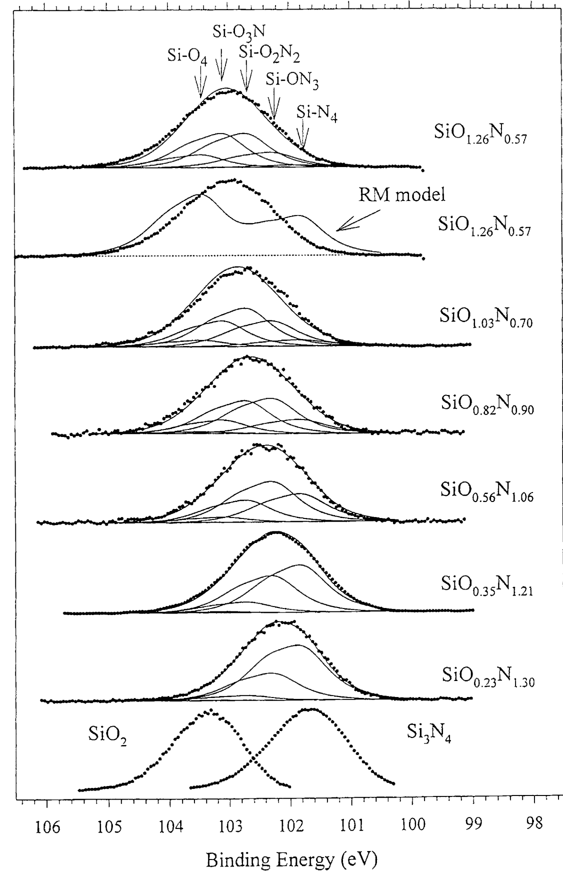

Fig. 1. Si 2p XPS spectra of SiO_xN_y with different compositions. The experimental spectra are shown in dots and the simulated spectra are depicted in solid lines.

Fig. 2 shows the Si 2p levels XPS of SiN_x with different compositions. The experimental spectra, the spectra simulated by RBM and the spectra simulated by RMM are shown in dots, dashed lines and solid lines, respectively. For SiN_x RBM simulation, the chemical shifts and values of FWHM of SiN_vSi_{4-v} ($v = 1, 2, 3$) tetrahedra were considered as linear functions of the number of nitrogen atoms. The experimental spectrum (first trace of Fig. 2) shows a feature dominated by two components. The RBM calculation predicts that the Si 2p spectrum consists of a single broad peak only and does not agree with the corresponding

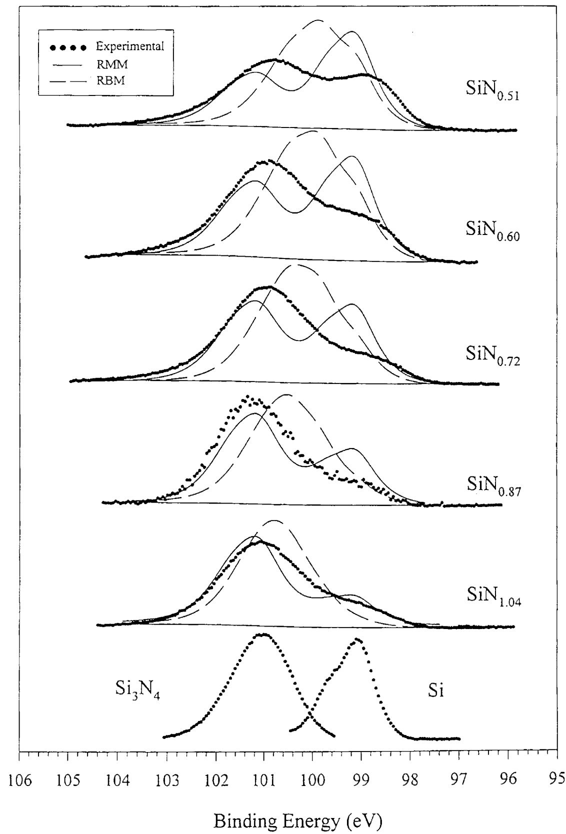

Fig. 2. Si 2p core level of SiN_x with different compositions. The experimental spectra, the spectra simulated by RBM and the spectra simulated by RMM are shown in dots, dashed lines and solid lines, respectively.

experimental spectrum. The first RMM Si 2p spectrum has two peaks corresponding to Si and Si_3N_4 phases and correlates quite well with the experimental spectrum in the peak locations. The XPS data show the existence of different chemical phases in SiN_x, corresponding to SiN_4, SiN_3Si, SiN_2Si_2, $SiNSi_3$, and SiN_4 tetrahedra. The existence of Si clusters for the present SiN_x samples has been reported previously using Raman scattering study [21]. The size of the Si cluster is estimated to be in the range of 1.5–5.0 nm. Previously, silicon clusters in SiN_x with size in the range 1.3–2.4 nm were observed directly with high-resolution transmission electron microscopy, photoluminescence, and optical absorption [22]. The sub-nitride components can be due to the species at the interfaces between the Si clusters and Si_3N_4. To have a better correlation to other experimental spectra, further de-convolution based on the mixture of Si, Si_3N_4 and sub-nitrides (SiN_3Si, SiN_2Si_2, and $SiNSi_3$ tetrahedra) is needed.

Depending on the chemical composition, the band gap for the SiN_x can vary from 4.6 ± 0.2 eV (nitride) to 1.1 eV (silicon) [15,23]. Hence the energy gap will fluctuate locally due to the spatial chemical composition fluctuations. The local gap fluctuations of the SiN_x result in spatial fluctuations of potentials for electrons and holes (see Fig. 3(a)). The XPS valence band spectra of Si_3N_4, Si, Au, and SiN_x samples had been measured to have quantitative information on the maximum of potential fluctuation for holes. Since the Si_3N_4 va-

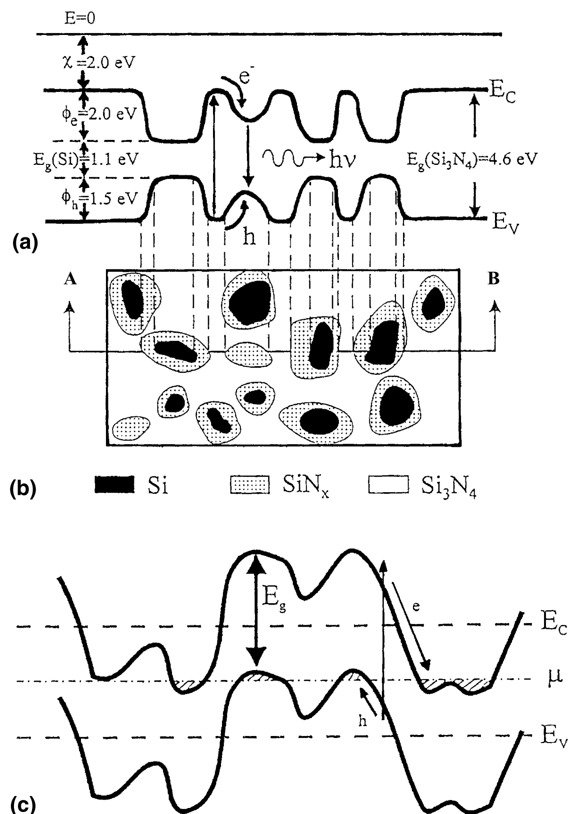

Fig. 3. Gigantic potential fluctuation model: (a) one-dimensional energy band diagram for SiN_x; (b) the corresponding spatial chemical composition fluctuation; and (c) the potential fluctuation model for highly doped compensated semiconductor.

lence band edge E_v is 1.5 ± 0.2 eV lower than that of Si [23] and the SiN_x valence band edge shifts towards the silicon band gap as the silicon content increases, the maximum value of hole potential fluctuation in SiN_x is 1.5 eV and the maximum value of electron potential fluctuation in SiN_x is equal to the electron barrier height $\Phi_e = 2.0 \pm 0.2$ eV at the Si/Si_3N_4 interface which was measured using internal photoemission and tunnel injection [8,15,23]. Based on these findings, a gigantic potential contra-variant fluctuations (GPF) model for SiN_x is developed and is depicted in Fig. 3(a). The qualitative model of GPF in SiN_x was discussed previously in [24,25] and in SiO_x in [12]. Note that Fig. 3(a) is the one-dimensional energy diagram for the cross-sectional view (AB line) of the local chemical composition fluctuation model in Fig. 3(b). In our GPF model for SiN_x, charge neutrality is maintained at every point in space. The local electric fields for electrons and holes at the same point are different in magnitude and opposite in direction. These gigantic contra-variant (for electrons and holes) potential fluctuations will cause non-equilibrium electron/hole pairs moving to the same spatial position with minimum energies. In addition, it results in excited carriers' confinement and increases the probability of carrier recombination. This phenomenon does not exist in SiO_xN_y with the RBM scenario. This model is similar to the gigantic potential co-variant fluctuation model for highly doped compensated semiconductor as shown in Fig. 3(c) [26,27]. However, the energy gap in the GPF model for highly doped compensated semiconductor is constant. The local electric field leads to carrier separation and local charge neutrality does not exist in this material.

4. Conclusion

In conclusion, XPS results show that the structure of SiO_xN_y film is not a mixture of SiO_2 and Si_3N_4 clusters. Instead, we found that the short-range order of SiO_xN_y film can be quantitatively described by the RBM. The SiO_xN_y constituted by the bonded networks comprises five sorts of randomly distributed tetrahedra SiO_vN_{4-v} (where $v = 0, 1, 2, 3$, and 4). With this connection, MOS devices with oxynitride as the gate dielectric will not induce gigantic surface potential fluctuations in the vicinity of the channel as no spatial local fluctuation of dielectric constant exists in the randomly distributed oxynitride tetrahedra. However, although silicon-rich SiN_x also comprises five tetrahedra, the distribution of these tetrahedra does not obey the RBM but the RMM. As a result, gigantic potential fluctuations in SiN_x occur due to the energy gap variation induced by spatial local chemical composition fluctuations.

Acknowledgements

This work is supported by project INTAS 97-0347 and partially by City U project no.: 7001134.

References

[1] D.A. Buchanan, IBM J. Res. Dev. 43 (1999) 245.
[2] C.S. Mian, I.S. Flora, Solid State Electron. 43 (1999) 1997.
[3] T.M. Pan, T.F. Lei, T.S. Chao, IEEE Electron Device Lett. 21 (2000) 378.
[4] Y.C. Yeo, Q.L. Lu, W.C. Lee, T.J. King, C. Hu, X. Wang, X. Guo, T.P. Ma, IEEE Electron Device Lett. 21 (2000) 540.
[5] J. Bu, M.H. White, Solid State Electron. 45 (2001) 113.
[6] V.A. Gritsenko, J.B. Xu, R.M. Kwok, Y.H. Ng, I.H. Wilson, Phys. Rev. Lett. 35 (1998) 1293.
[7] S. Hasegawa, S. Sakamori, M. Futsudera, T. Inokuma, Y. Kurata, J. Appl. Phys. 89 (2001) 2598.
[8] V.A. Gritsenko, N.D. Dikovskaja, K.P. Mogilnikov, Thin Solid Films 51 (1978) 353.
[9] H.R. Philipp, J. Non-Cryst. Solids 8–10 (1972) 627.
[10] S. Hasegawa, L. He, T. Inokuma, Y. Kurata, Phys. Rev. B 46 (1992) 12478.
[11] R. Karcher, L. Ley, R.L. Johnson, Phys. Rev. B 30 (1984) 1896.
[12] V.A. Gritsenko, Yu.P. Kostikov, N.A. Romanov, JETP Lett. 34 (1981) 3.
[13] I.A. Britov, V.A. Gritsenko, Yu.N. Romaschenko, Sov. Phys. JETP 62 (1985) 321.
[14] V.A. Gritsenko, Yu.P. Kostikov, S.P. Sinitsa, Inorg. Mater. 19 (1983) 408.
[15] V.A. Gritsenko, in: Silicon Nitride in Electronics, Elsevier, New York, 1988.
[16] Z. Yin, F.W. Smith, Phys. Rev. B 42 (1990) 3658.
[17] G. Wiech, A. Simunek, Phys. Rev. B 49 (1994) 5398.
[18] T.S. Eriksson, C.G. Granqvist, J. Appl. Phys. 60 (1986) 2081.

[19] A. Sassella, Phys. Rev. B 48 (1993) 14208.
[20] R.T. Sanderson, in: Chemical Bonds and Bond Energy, 2nd Ed., Academic, New York, 1976, p. 77.
[21] V.A. Volodin, M.D. Efremov, V.A. Gritsenko, I.A. Kochybei, Appl. Phys. Lett. 73 (1998) 1212.
[22] N.M. Park, C.J. Choi, T.Y. Seong, S.J. Park, Phys. Rev. Lett. 86 (2001) 1355.
[23] V.A. Gritsenko, E.E. Meerson, Yu.N. Morokov, Phys. Rev. B 57 (1997) R2081.
[24] M. Yamaguchi, C. Ogihara, H. Ohta, K. Morigaki, J. Non-Cryst. Solids 114 (1989) 705.
[25] K.C. Lin, S.C. Lee, J. Appl. Phys. 72 (1992) 5474.
[26] B.I. Shklovskii, A.I. Efros, Sov. Phys. JETP 35 (1972) 610.
[27] B.I. Shklovskii, A.I. Efros, Electronic Properties of Doped Semiconductors, Science, Leningrad, 1979.